

Impact Properties of Adult and ATD Heads

Andre Matthew Loyd, Roger W. Nightingale, Yin Song, Jason F. Luck, Hattie Cutcliffe, Barry S. Myers, Cameron 'Dale' Bass

Abstract Traumatic brain injury (TBI) causes 1.1 million trips to the hospital each year in the US, with 235,000 of these injuries requiring admissions. Given the importance of TBI, head injury has been studied extensively using both cadavers and anthropomorphic test devices (ATDs). However, few studies have benchmarked the response of ATD heads against human data.

The goal of this study was to investigate the response of the adult and ATD heads in impact, and to compare ATD and human responses. In this study, six adult heads and seven ATD heads were used to obtain impact properties. The heads were dropped from 15cm and 30cm onto five impact locations.

No statistical differences were found between the adult human heads and the adult Hybrid III head for 15cm and 30cm rigid surface impacts ($p < 0.05$). For the human heads, the mid-sagittal impact locations produced the highest HIC and peak acceleration values. The parietal impacts were found to produce HICs and peak accelerations that were 26% to 48% lower than the mid-sagittal impacts. For the ATD heads, the acceleration and HIC generally increased with represented age, except for the Q3, which produced the HIC values up to 56% higher than the other heads.

Keywords ATD; head impact; Hybrid III; head injury; Traumatic brain injury

I. INTRODUCTION

Traumatic brain injury (TBI) is one of the major causes of injury and death in the United States. It is estimated that 1.7 million people report a head injury every year in the US; of those, 275,000 will be hospitalized and 52,000 will die -- making head injury responsible for 30% of all injury deaths [1]. Of these, motor vehicle crashes are responsible for 294,000 brain injuries and 16,500 deaths. Financially, the burden of TBI in the United States is more than a billion dollars per year in direct patient expenses [2].

One of the main tools used to study head injury are anthropomorphic testing devices (ATDs). ATDs simulate the human head geometry and impact response. One ATD widely used in automotive impact testing is the 50th percentile Hybrid III adult male, henceforth referred to as adult Hybrid III [3]. It has been in use since the 1970s and is currently used in standards for evaluating the safety of cars [4, 5]. Other ATDs have been developed to evaluate the safety of child restraint systems and cars, including ATDs representing an average anthropometry for pediatric ages from age newborn to 10-year-old [6, 7]. The adult Hybrid III was benchmarked against forehead skull fracture data; however, the other child ATD heads and the other locations on the adult Hybrid III head have not been compared against human data [4, 8, 9].

Most TBIs occur from direct head impacts onto other objects. Drop tests, with prescribed impact momentum and location, are a controlled way of mimicking these impacts and are the current method for validating the response of ATDs [4, 10]. From drop tests, the response of the heads can be analyzed to understand impact properties and the head can be characterized in impact. To correctly characterize the impact properties of the adult and ATD heads, this study will evaluate the impact response of the human adult head and seven different ATD heads. The results will characterize the impact response of the adult head for five different impact locations, and quantify the changes in response of the ATD head with represented age. In addition, the Hybrid III will be directly evaluated against the adult head for multiple impact locations.

Andre Loyd is a post-doctoral fellow in the Department of Orthopedic Surgery at the Mayo Clinic ((507)-284-9298 Email: andrel@alumni.clemson.edu Fax: (507)-284-5392). B. S. Myers, R. W. Nightingale, D. Bass are professors of Biomedical Engineering at Duke University. J. Luck and H. Cutcliffe are graduate students at Duke University. Y. Song was an engineer in the Biomedical Engineering Department at Duke University.

II. METHODS

Two sets of heads were tested: six adult cadaver and seven ATD heads (Table 1 and Table 2). The cadaver drop tests were performed following a neck testing series and prior to a head compression test series [11]. The cadaver heads were dissected from the neck at the atlanto-occipital joint. The mandibles of all specimens had been removed during the prior neck testing and remained detached for all head drop tests. The head circumferences, lengths, and widths were measured. Both external auditory meatuses (EAMs) were marked with pins, as were both infraorbital foramen (IOF), while the Frankfort plane was marked with a line drawn from the EAM to the IOF using a Sharpie pen [12]. Each head was filled with saline (0.9% NaCl solution) to remove all air voids. Then the heads were sealed at the occipital condyles with polymethylmethacrylate (PMMA) to contain all intracranial contents during the head drop tests. Markers were placed randomly on each head to enable motion tracking. Finally, each head was weighed to determine head drop mass.

Table 1: Adult heads used in the head impact tests.

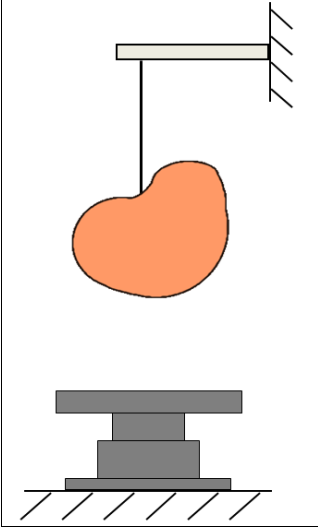
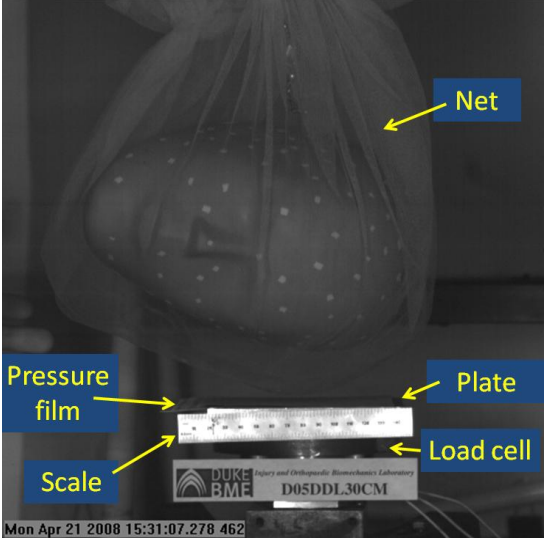
Specimen ID	Age	Sex	Race	Cause of death	Head drop mass (kg)
A01M	61-years-old	M	Caucasian	Unknown	3.16
A02M	53-years-old	M	Caucasian	Respiratory failure	3.27
A04M	59-years-old	M	Hispanic	Septic shock	3.21
A05M	58-years-old	M	Caucasian	Chronic obstructive pulmonary disease	3.08
A06M	67-years-old	M	Caucasian	Respiratory failure	3.41
A07M	67-years-old	M	Caucasian	Unknown	3.45

Table 2: ATD heads used in the head impact tests.

Specimen ID	ATD head	Head drop mass (kg)
D01D	50 th percentile adult male Hybrid III	4.32
D02D	12-month CRABI	2.65
D03D	3-year Hybrid III	2.50
D04D	6-year Hybrid III	3.30
D05D	10-year Hybrid III	3.74
D06D	3-year-old Q3	2.81
D07D	6-month CRABI	2.10

The drop tests were performed using two drop heights, 15cm and 30cm, and onto five impact locations: right and left parietal, forehead, occiput and vertex. One set of drops was performed on the post mortem human subject (PMHS) heads while up to four sets of drops were carried out on the ATD heads. The repeated drops for each ATD head were done using the same ATD, and there was at least an hour of wait time between impacts onto the same impact location for each ATD. For each drop, the head was placed into a fine net that was attached to a pulley using nylon line (Figure 1 and Figure 2). The head was positioned inside the net to set the desired impact location. The head was then adjusted to the desired drop height and released by burning the nylon line, which allowed free fall without rotation or out-of-plane translation. The head then impacted a smooth, flat aluminum platen that was 3/4-inches thick and attached to a Kistler 3-axis piezoelectric load cell (Kistler, France) (Figure 1), which was rigidly bolted to a structural floor. A Pressurex® (Sensor Products Inc., Madison, NJ) pressure sensitive film was placed on top of the platen to capture the contact area. Force-time data were recorded using LabVIEW (National Instruments, Austin, TX) at a sample rate of 100,000 Hz. A Phantom high-speed digital video camera (Vision Research, Inc., Wayne, NJ) recorded all of the head drops at a frame rate of 2,000 frames per second.

For analysis, all data were filtered using the SAE J211b Class 1000 filter specifications for head impact [13]. Peak resultant acceleration, head injury criterion (HIC) and impact stiffness were calculated for each head drop. The acceleration time history was estimated by dividing the force time history by the drop mass and was used to calculate peak resultant acceleration and HIC [14]. The duration of the impact was set by the time points at which the force time history crossed 0.1% of the full range of the force.

	
<p>Figure 1: Schematic of head drop setup.</p>	<p>Figure 2: The head drop setup during a head impact. The head in this figure is the 10-year-old Hybrid III.</p>

Force/displacement curves were obtained by double integrating the acceleration time histories to calculate displacement and using the force from the force/time curves. To calculate impact stiffness, the force and calculated displacement curve were combined to make a force/displacement curve. Linear regression from 50% of the peak displacement to peak force was used to calculate the impact stiffness. Analysis of covariance (ANCOVA) was used for statistical analyses of drop height and impact location on HIC, peak resultant acceleration and impact stiffness with $p < 0.05$. To test for significant differences between impact locations, the Tukey-Kramer method was used with a significance level of $p < 0.05$. The significant difference between the drop heights for the human heads was found using the ANCOVAs. Levene tests were performed for each ANCOVA to ensure that the variances were equal and that use of the ANCOVA was valid ($p > 0.05$).

Because the ATD heads had repeated drops, repeated-measures analyses of covariance were used to investigate the significance of the ATD head, drop height and impact location on HIC, peak resultant acceleration and impact stiffness. The equality of the variances (or the sphericity) was found using Mauchly's sphericity test to ensure that it was valid to use repeated-measures ANCOVA ($p > 0.05$). If the variables lacked sphericity ($p < 0.05$), a multivariate analysis of covariance F-test was done [15]. Student t-tests were used to test for differences between drop heights for drops on the same location for the same ATD head.

The adult heads and the 50% percentile adult Hybrid III male head were compared directly by comparing the peak resultant acceleration, HIC and impact stiffness of each head drop. The adult and adult Hybrid III heads were compared using generalized linear models with a significant difference level of $p < 0.05$.

III. RESULTS

Adult Heads

Acceleration

The ANCOVA analysis for the peak acceleration showed that the impact location ($p < 0.0001$) and drop height ($p < 0.0001$) were all significant predictors of the peak acceleration. The Levene tests showed that the variances were equal and therefore that use of the ANCOVA was valid ($p > 0.05$). For the impact location in adults, the vertex had the statistically highest response and the parietal impacts had the statistically lowest response, according to Tukey-Kramer tests following the ANCOVA ($p < 0.018$) (Figure 3).

Figure 3 illustrates the effect of drop height and impact location on acceleration. These effects were consistent across the adult heads and all impact locations.

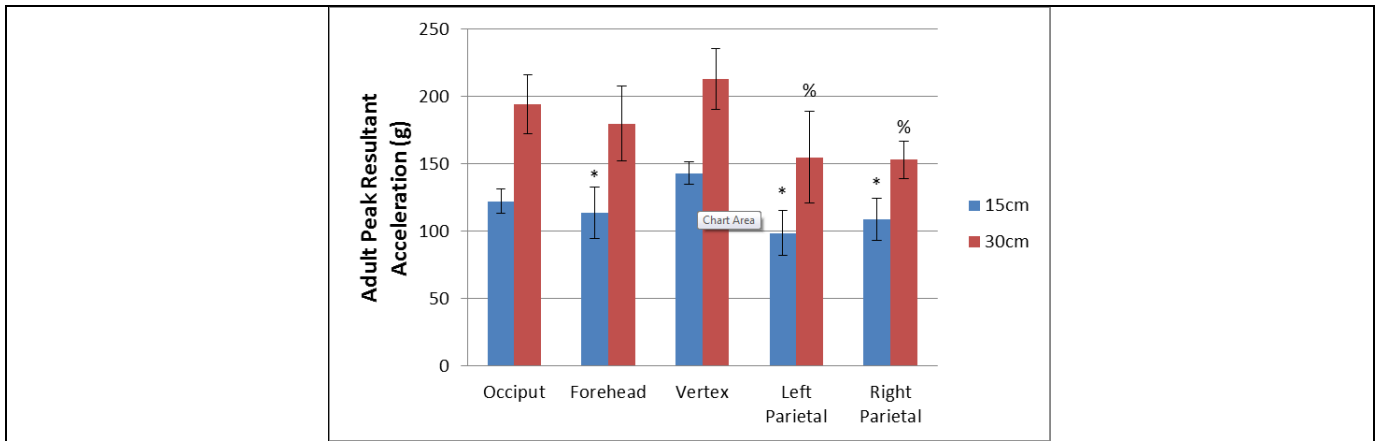


Figure 3: Average adult peak resultant acceleration by drop location. % denotes that the impact location is significantly different from the vertex 30cm drop (ANCOVA with post-hoc Tukey-Kramer tests $p < 0.018$) while * denotes that the impact location is significantly different ($p < 0.005$) from the vertex 15cm drops.

HIC

The results for HIC were analyzed using analysis of covariance. These results mirror the peak acceleration results, as the ANCOVA showed that both drop height ($p < 0.0001$) and impact location ($p < 0.0001$) were significant predictors of the HIC. For the impact location of the adult heads, the vertex ($p < 0.0247$) produced the statistically highest HIC values, while parietal impacts produced the statistically lowest HIC values according to the Tukey-Kramer method. Levene tests further showed that the variances were equal and that use of the ANCOVA was valid ($p > 0.05$) in these analyses. The influences of impact location and drop height on the HIC are illustrated by Figure 4 and Figure 5. Both indicate that an impact at the vertex produced the highest HIC values and that parietal impacts produced the lowest HIC values.

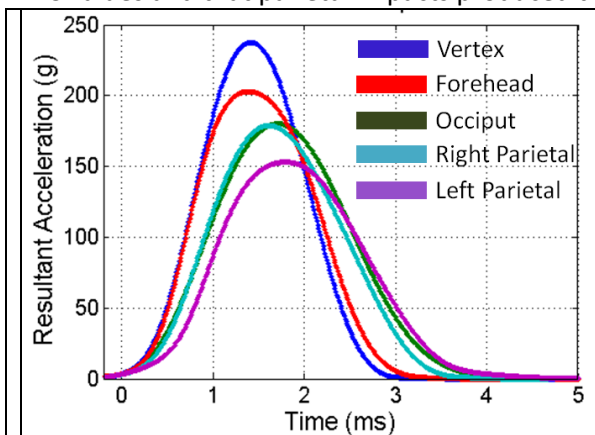


Figure 4: Example acceleration-time pulse for an adult head (A01M) for all 30cm impact locations. Statistically, the drops onto the vertex had the highest HICs and peak resultant accelerations while the parietal drops had the lowest HICs and peak resultant accelerations for adult head impacts (ANCOVA with post-hoc Tukey-Kramer tests $p < 0.05$).

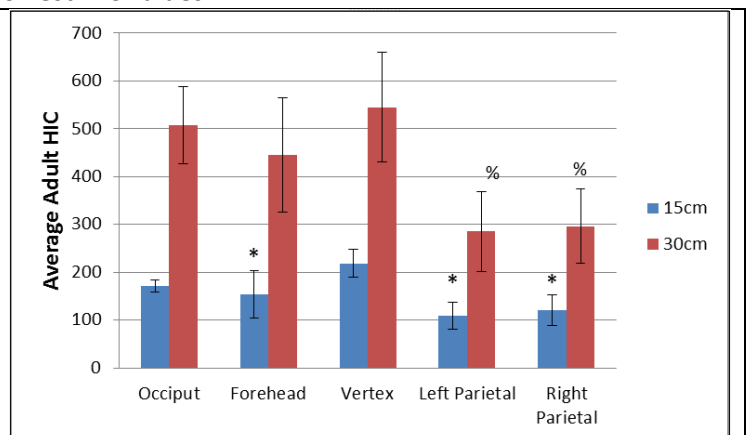


Figure 5: Average HIC for the adult heads by impact location, showing the HIC's dependence on impact location. * denotes that the drop is statistically different from the 15cm vertex HIC (ANCOVA with post-hoc Tukey-Kramer tests $p < 0.0247$). % denotes that the drop is statistically different from the 30cm occiput and vertex HICs (ANCOVA with post-hoc Tukey-Kramer tests $p < 0.0018$).

Impact Stiffness

An ANCOVA showed that drop height ($p = 0.009$) and impact location ($p < 0.0001$) were significant predictors for the impact stiffness of the human head impacts. The ANCOVA showed that the impact stiffness of the parietal drops were statistically lower than the impact stiffness of the vertex drops, while the impact stiffness of the 15cm drops were statistically lower than those of the 30cm drops. Levene tests showed that the variances were equal and that ANCOVA was valid to use in this analysis ($p > 0.05$).

The effect of impact location is illustrated in Figure 6, where the Tukey-Kramer method showed that parietal impacts were statistically different from the vertex impact for the 30cm drops.

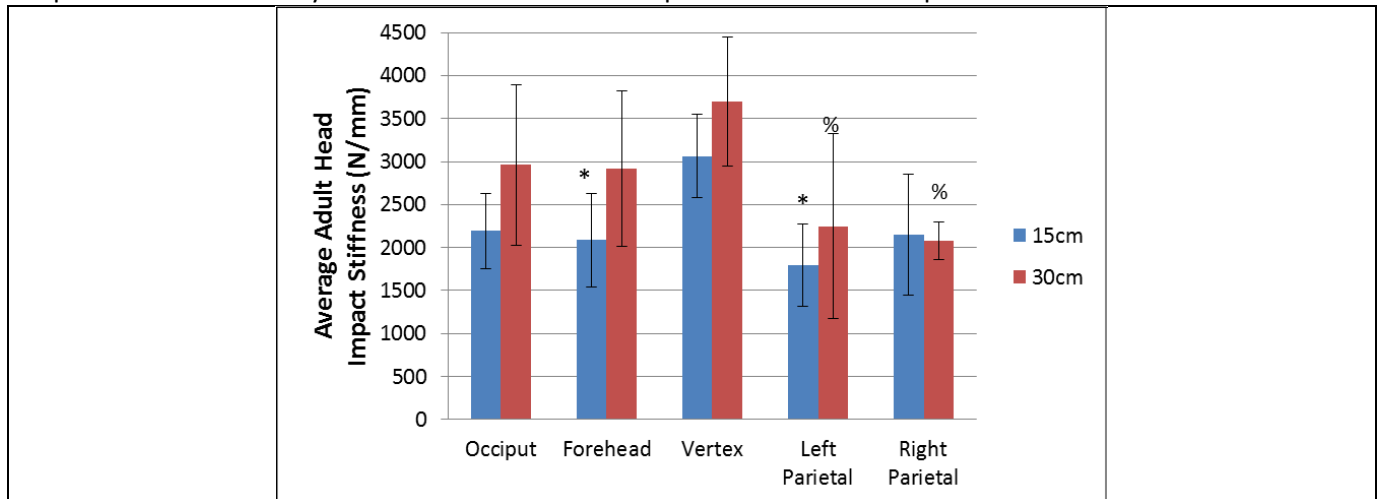


Figure 6: Average adult head impact stiffness for each impact location. The parietal impacts were statistically lower than the other impact locations. * denotes that the average impact stiffness was statistically different ($p < 0.0332$) from the average 15cm vertex impact stiffness (ANCOVA with post-hoc Tukey-Kramer tests $p < 0.034$). % denotes that the average impact stiffness was statistically lower than the average 30cm vertex impact stiffness (ANCOVA with post-hoc Tukey-Kramer tests $p < 0.042$).

ATD Heads

Acceleration

The results for the ATD non-destructive impacts were analyzed using repeated-measures ANCOVA. The repeated-measures ANCOVA showed that the peak resultant acceleration was not affected by the repeated tests ($p = 0.324$); however, it did show that the drop height and ATD head were significant predictors of resultant acceleration ($p < 0.04$). Impact location was not significant, but was trending to be significant ($p = 0.051$). Mauchly’s sphericity test showed the resultant acceleration variances were equal, confirming the repeated-measures ANCOVA results ($p = 0.99$).

For each ATD head, the individual repeated measures ANCOVA showed that drop height was always a significant indicator of resultant acceleration and that impact location was a significant indicator for five of the seven ATD heads ($p < 0.05$). The 10-year-old Hybrid III and the 6-year-old Hybrid III resultant accelerations were not significantly dependent on impact location (Table 3) (Repeated-measures ANCOVA $p > 0.05$). The 3-year-old Q3-dummy produced the highest resultant acceleration for the majority of the drops; likewise, the 6-month CRABI and 12-month CRABI produced the lowest resultant acceleration in all of the tests (Figure 7 and Table 3). The resultant acceleration consistently increased with drop height for all impact locations and all ATD heads.

A table of how the ATD heads differ from each other is shown in Table 3. The table indicates that the 3-year-old Q3 dummy had the highest accelerations for two of the five drops and that the CRABI ATDs produced the lowest accelerations for all of the drops. The table also shows that the occiput was the location that was statistically different for all ATDs, according to the Tukey-Kramer method ($p < 0.05$) (Table 3).

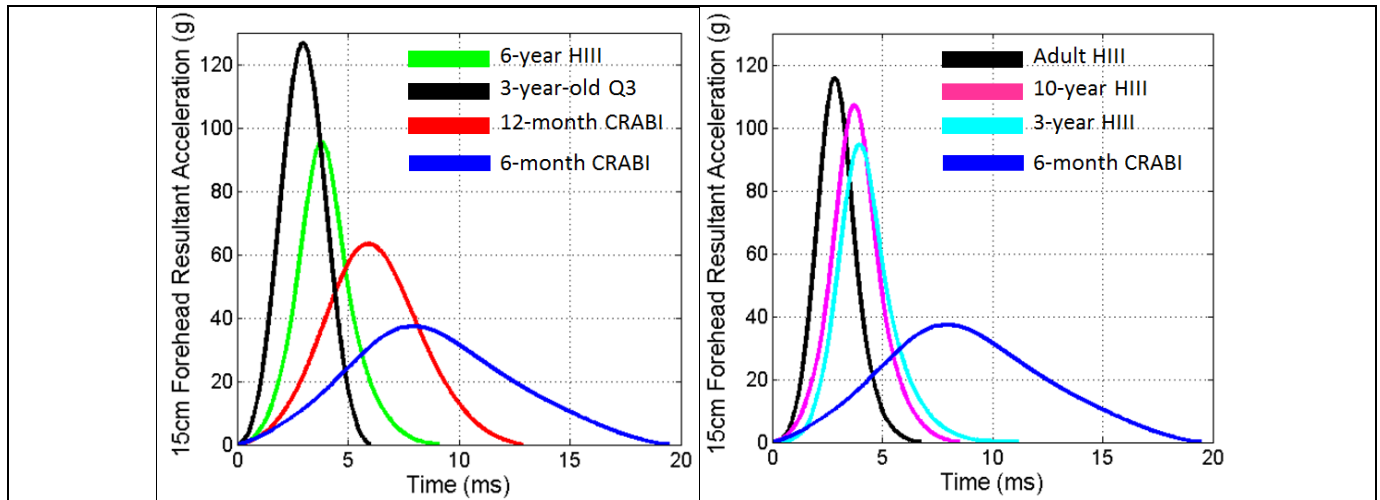


Figure 7: 15cm forehead resultant accelerations for all ATD heads. The 3-year-old Q3 dummy had the highest resultant acceleration and the shortest pulse duration. The 6-month CRABI had the lowest resultant acceleration and longest pulse duration.

Table 3: The average peak resultant acceleration (g) for the 30cm impacts for the ATD heads. Peak acceleration was statistically dependent on the ATD being tested and the drop height (repeated-measures ANCOVA $p < 0.05$). The 3-year-old Q3 had the overall highest peak resultant acceleration for two of the five locations for the 30cm impacts. The 6-month and 12-month CRABIs had the lowest resultant accelerations for each 30cm impact location. The occiput was statistically different from the other locations for each ATD head, whether lower or higher (multiple Tukey-Kramer tests). The red numbers indicates the highest values and the blue numbers indicates the lowest values.

ATD head	Drop Height	Vertex	Occiput	Forehead	Right Parietal	Left Parietal
6-month CRABI	30cm	52	62	85	145	214
12-month CRABI		86	56	110	106	117
3-year HIII		169	83	160	142	154
3-year-old Q3		234	255	203	174	181
6-year HIII		184	218	174	209	190
10-year HIII		230	285	193	197	207
Adult HIII		208	235	189	174	166

HIC

A repeated-measures ANCOVA showed that drop height, impact location, and ATD head were all significant predictors of the head injury criteria ($p < 0.04$). The repeated drops were not shown to affect the HIC ($p > 0.26$). A Mauchly’s sphericity test showed that the variances were equal and that use of the repeated-measures ANCOVA was valid ($p > 0.96$).

The 3-year-old Q3 drops produced the highest HIC values for all impact locations and drop heights (Table 4). The 6-month CRABI and 12-month CRABI had the lowest HIC for the majority of the impacts (Table 4). Tukey-Kramer mean comparisons were performed for the impact locations for each specimen, and the occiput and parietal impacts were shown to be statistically different for most of the drops. For all ATDs and impact locations the HIC increased with increasing drop height (Table 4).

Table 4: Average HIC values for the each ATD head for the 30cm impacts. The 3-year-old Q3 produced the highest HIC values for all 30cm head impacts, while the 6-month CRABI, 12-month CRABI and 3-year-old HII produced the lowest HIC values for the 30cm head impacts. The red numbers indicates the highest values and the blue numbers indicates the lowest values.

ATD head	Drop Height	Vertex	Occiput	Forehead	Right Parietal	Left Parietal
6-month CRABI	30cm	99	126	157	301	488
12-month CRABI		200	106	262	237	270
3-year HIII		348	131	341	227	268
3-year Q3		931	977	707	516	561
6-year HIII		430	499	407	409	355
10-year HIII		598	697	469	355	387
Adult HIII		535	644	458	323	291

Impact Stiffness

The repeated-measures ANCOVA analysis of the ATD impact stiffness showed that the ATD impact stiffness was dependent on the ATD head ($p < 0.0001$), impact location ($p = 0.03$) and drop height ($p < 0.0001$). The repeated measures did not affect the impact ($p = 0.56$) and Mauchly’s sphericity test did not show any level of unequal impact stiffness variance ($p = 0.50$), confirming use of a repeated measures ANCOVA was valid.

Overall, the Adult Hybrid III had the highest dynamic stiffness while the 6-month-old CRABI had the lowest stiffness (Table 5). As illustrated by Table 5, the dynamic stiffness generally increased with increasing represented age. Only the 3-year-old Q3 did not follow this pattern. Likewise, the dynamic stiffness increased with drop height in all cases (Table 5). No distinct relationship between impact location and stiffness was identified across all heads. Impact locations that were statistically different from all other impact locations were identified for the 3-year-old HIII, 3-year-old Q3 and the 10-year-old HIII using the Tukey-Kramer method ($p < 0.05$). This was not true for the CRABIs or the 6-year-old and Adult Hybrid IIIs ($p > 0.05$). The highest impact stiffness was found to be 5110 N/mm for the 30cm occipital drop for the 10-year-old HIII, while the lowest was 95 N/mm for the 15cm vertex drop for the 6-month CRABI.

Table 5: The average impact stiffness (N/mm) for the 30cm drops for the ATD heads. The impact stiffness was dependent on the ATD head, impact location and drop height. The adult Hybrid III, 10-year-old Hybrid III, and the 3-year-old Q3 produced the highest impact stiffness for the 15cm drops. The 6-month and 12-month CRABIs produced the lowest impact stiffness for the 30cm drops. The red numbers indicates the highest values and the blue numbers indicates the lowest values.

ATD head	Drop Height	Vertex	Occiput	Forehead	Right Parietal	Left Parietal
6-month CRABI	30cm	114	143	312	899	2109
12-month CRABI		360	160	575	613	723
3-year HIII		1570	432	1277	1345	1408
3-year Q3		2620	3370	2041	1601	1706
6-year HIII		1999	3335	1670	3203	2540
10-year-old HIII		3406	5112	2314	3225	3850
Adult HIII		3762	3342	3005	3258	2995

Hybrid III-Adult Head Comparison

The adult heads and the adult Hybrid III impact responses were mostly in agreement for all of the comparisons. For the resultant acceleration comparison, the generalized linear model using head type (adult or Adult Hybrid III), impact location and drop height as the independent variables showed that there was no statistical difference between the adult heads and the adult Hybrid III heads ($p = 0.25$) (Figure 8). The differences for each impact location ranged from 5% to 21%, with the largest difference seen in the 30cm occipital impact.

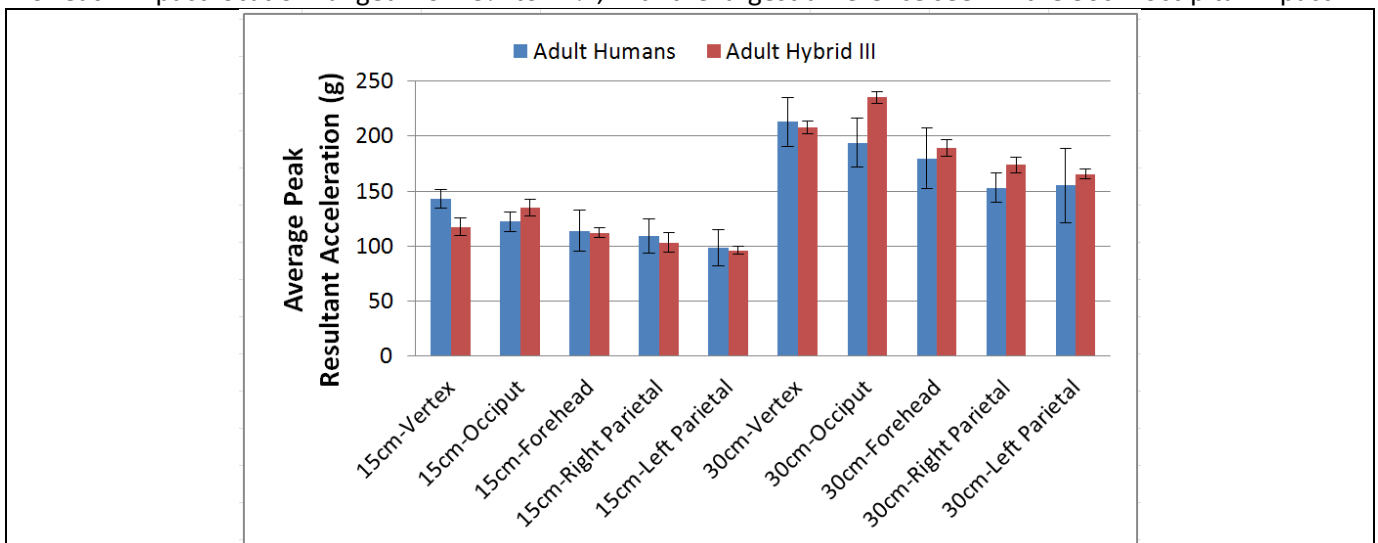


Figure 8: Average peak resultant accelerations of the adult Hybrid III and the adult heads (n=6). The adult heads and the adult Hybrid III values are not statistically different according to a generalized linear model using head type (adult or Hybrid III), impact location, and drop height as the independent variables ($p = 0.25$).

For HIC, the adult heads and the adult Hybrid III head were not statistically different, according to a generalized linear model using head type, impact location, and drop height ($p=0.41$). The largest differences in drops ranged from 24%-27%. The HIC of the 30cm occipital impact had the largest difference at 27%. The forehead drops resulted in HIC values that were the most similar between the adults and the Hybrid III, with the differences between the HIC values for the 15cm and 30cm impacts being 1% and 3%, respectively.

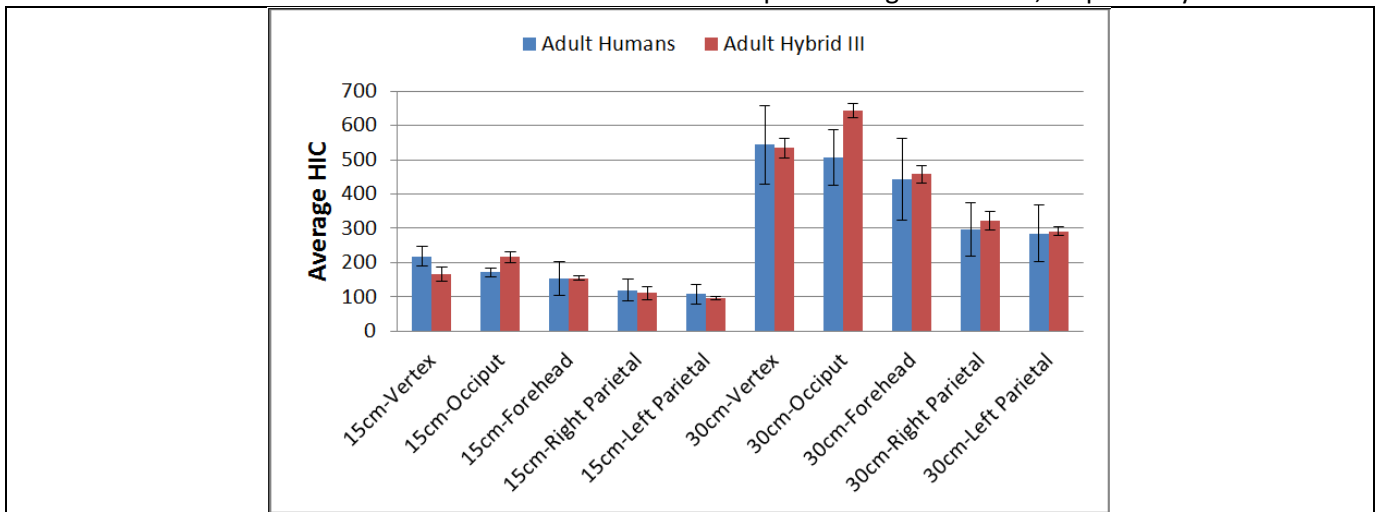


Figure 9: HIC values of the adult Hybrid III and the adult heads (n=6). A generalized linear model showed that the adult heads and the Hybrid III heads were not statistically different for HIC response during 15cm and 30cm impacts ($p=0.41$).

The adult impact stiffness values were not statistically different from the adult Hybrid III's values according to a generalized linear model using head type, impact location and drop height ($p=0.12$) (Figure 10). The most different stiffness values resulted from the 15cm vertex impact and the 30cm right parietal impact. The forehead impacts had the most similar stiffness values between the adult heads and the adult Hybrid III, with differences of 1% and 3% for the 15cm and 30cm impacts, respectively (Figure 10).

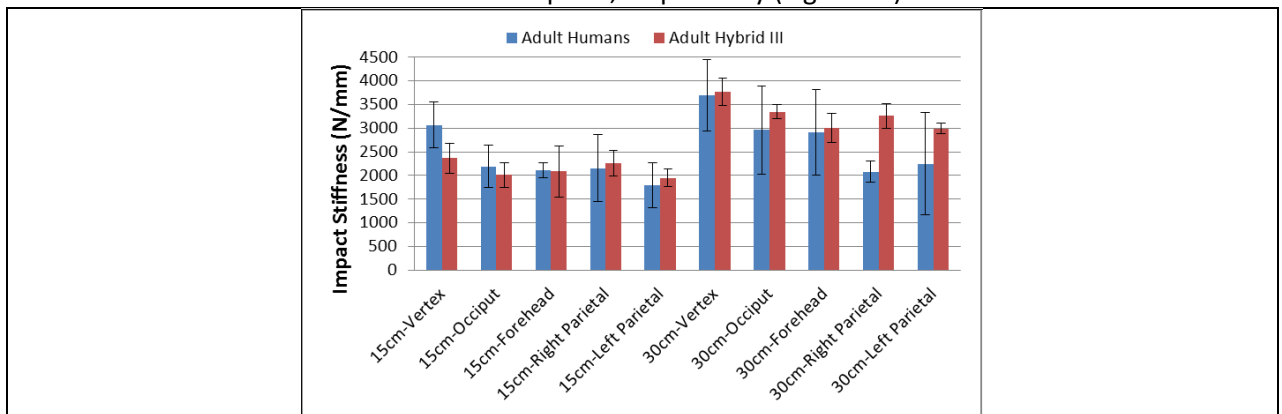


Figure 10: Impact stiffness values for the adult Hybrid III and the adult heads (n=6). The adult head and the adult Hybrid III head were not found to be statistically different, according to a generalized linear model ($p=0.12$).

IV. DISCUSSION

The goal of this study was to investigate the impact properties of adult and ATD heads using rigid plate impacts. Dynamic variables including the peak acceleration, HIC and impact stiffness were used to assess the response of ATD heads and the impact properties of the Hybrid III were directly compared against those of the adult heads for rigid plate impacts. The results indicate that the Hybrid III is an adequate representation of the adult, and that ATD heads follow the general trend of increasing in acceleration with age, with the 3-year-old Q3 being the lone exception. Additionally, it was shown that the response of all heads was significantly dependent upon the impact location and drop height.

Previous studies of impact include tests with the head attached to the neck in which an impactor strikes the head of a whole cadaver, as well as drop tests in which a complete cadaver or a head and neck system are dropped together [16-18]. However, the current study has the advantage of an isolated head in free-fall, experiencing no translational or rotational motion before impact. This insures that the impact of the head is evaluated without the coupling effects of the neck, and that all of the energy of the impact is absorbed by the head [19]. The rigid surface of impact and the one-dimensional motion of the head represent simplified boundary conditions that are useful for finite-element or lumped-mass model validation [20, 21]. In addition, the technique used in this study is similar to the current certification test as set by the National Highway Traffic Safety Administration for the Hybrid III and child ATDs [4]. However, one potential concern in conducting these tests is that air voids in the skull may allow secondary impacts between the brain and the inside of the skull, which would be seen in the data as two peaks in the acceleration time histories. This issue was avoided in the current study by perfusing saline into the foramen magnum to remove any air voids, forcing the brain and cerebrospinal fluid to be in contact with the inner table of the skull during impact [22] and eliminating any potential for secondary impacts.

The most similar dataset to that of the current study is the work conducted by Hodgson and Thomas [17]. They conducted a series of head drop experiments, in which entire embalmed bodies were dropped onto the forehead from 25.4mm (10 inches) [17]. Since the head is not coupled to the rest of the body during the Hodgson and Thomas impacts, the head mass and peak load cell force were used to calculate peak resultant accelerations (Figure 11) [23, 24]. No statistical difference was found between the Hodgson and Thomas 25.4mm forehead impacts and the 30cm adult forehead impacts of the current study. The 25.4mm drops showed slightly lower response values, but this is likely due to the slightly lower drop height. The Hybrid III was found to be in agreement with these two datasets, as it averaged a peak acceleration of 189g for the 30cm forehead drops, a 5% difference from the accelerations of the current study.

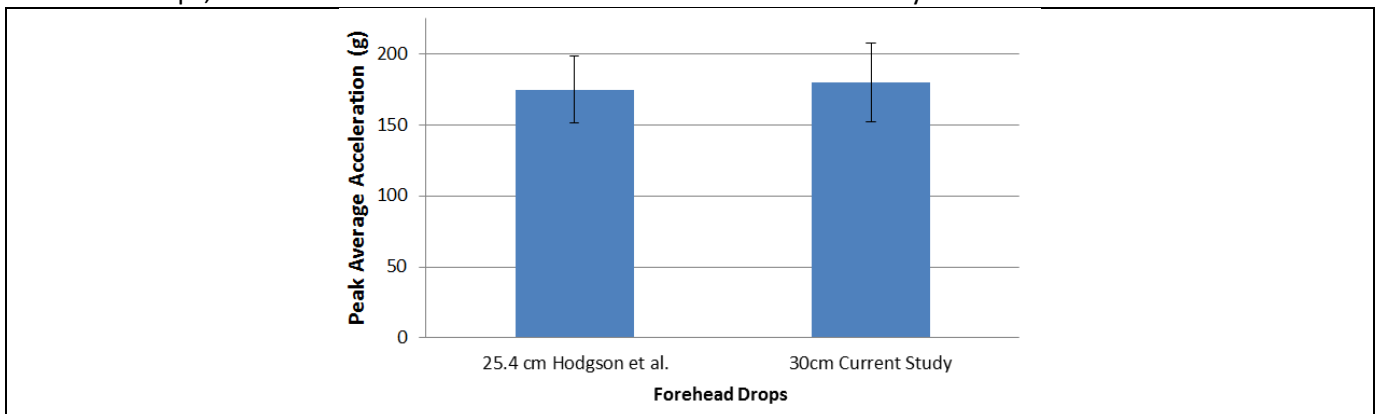


Figure 11: Peak resultant accelerations of head impacts of Hodgson and Thomas and of the current study. The Hodgson drops were from 25.4cm onto the forehead, while the current drops were from 30cm onto the forehead [17]. The 25.4cm forehead impacts and the 30cm forehead impacts are not statistically different.

ATD Representation

The adult Hybrid III response matched the response of the human heads with no statistical differences for rigid impacts from drop heights of either 15cm or 30cm. The forehead of the adult Hybrid III was particularly accurate, as it averaged a 4% error for the peak acceleration and 2% error for the impact stiffness and HIC. This accuracy is because the Hybrid III was designed using forehead impact data [3]. For the other impact locations, average errors of the Hybrid III were 10%, 13%, and 18% for peak acceleration, HIC and impact stiffness, while the average percentage standard deviations of the adult heads were 12%, 21% and 26% for the same drops. This shows that the adult Hybrid III produces very accurate responses for impacts onto the forehead and adequate responses for impacts onto the other locations. This confirms the Hybrid III head for forehead impacts at drop heights below the current 37.6cm head drop design specification, and shows that the Hybrid III head can give useful data, given that the errors are taken into account, for impacts onto the occiput, vertex and parietal impact locations for drop heights under 30cm [9].

The drops for all ATDs showed a very high level of repeatability. The ATDs averaged less than 6% variation in peak acceleration in repeated drops onto the same impact location and the same drop height. Generally, the HIC and peak acceleration properties of the ATD increased with the designed-age of the ATD, with the exception of the 3-year-old Q3. This is expected since scaling rules, used to develop ATDs of non-adult ages, prescribe

that the acceleration of the head increases with an increase in head size [25, 26]. However, the Q3 produced HIC and peak average resultant acceleration values that were higher than those of the Hybrid III adult (Table 3) and the adult heads. This is in contradiction to the neonatal data showing that the acceleration decreases with age [27].

Effect of Impact Location

The impact location was shown to be a significant variable for all impact properties for all heads. This makes the head impact location one of the most important factors influencing the impact response of the head. A survey of the mechanical properties demonstrates that the vertex produced the highest values for acceleration, HIC and dynamic stiffness, while the parietal produced the lowest values for the same properties (Figure 5 and Table 4). This difference is largely due to differences in anatomy and head kinematics during impact for each impact location.

The anatomical differences in skull thickness anatomy lead to the differences in impact response across different impact locations. A review of the literature indicates that each of the adult impact locations had a different skull thickness (Table 6) [28-30]. The impact region that averaged the highest skull thickness from the literature (the vertex) produced the highest acceleration, HIC and dynamic stiffness values. In descending order, the vertex, midline of the frontal bone and the lambda (the junction of the two parietal bones and the apex of the occipital bone) had the largest thicknesses and their impact properties denote that they were the locations with the stiffest response. The opposite was true for the parietal impacts, as they had the lowest thicknesses, and consequently the lowest acceleration, HIC and impact stiffness values. This could mean that the thinner regions of bone cause the head to have a less stiff response for an impact onto that region, while the thicker regions cause the head to have a more stiff response.

Table 6: Thickness measurements reported in the literature for different locations of the adult skull.

Skull location	Skull thickness (mm)	Reference
Midline frontal bone	7.044	[30]
Vertex ⁺	7.2-7.4	[28]
Lambda	6.9	[29]
Parietals at the euryons	5.04	[30]
Parietal eminences	4.7	[29]
Frontal eminences	4.0	[29]

+ Denotes a measurement of apex of the parietal bone.

The second reason for the differences across impact locations was the kinematics. For the vertex drops, the impact location was in the line of action of the center of gravity (CG), as illustrated by the lack of rotation of the head after impact (Figure 12). This caused higher accelerations and higher HIC values to be seen in impacts onto the vertex. Conversely, for the parietal impacts, the CG of the head was not in the line of action of the resultant force. This was evidenced by the large amount of rotation seen in the impact videos as well as by the lower acceleration and HIC values. This oblique loading effect was also present in the ATD impacts, where the ATD parietal impacts had statistically lower acceleration and HIC values because energy was transferred from one-dimensional linear motion to rotational motion (Figure 5, Figure 6, and Table 4). This effect has also been seen in a previous study of helmet impacts, where more oblique impacts had lower HICs and peak accelerations [31]. An example of this effect is shown in the differences between the right parietal and vertex adult Hybrid III 30cm drops (Figure 12).

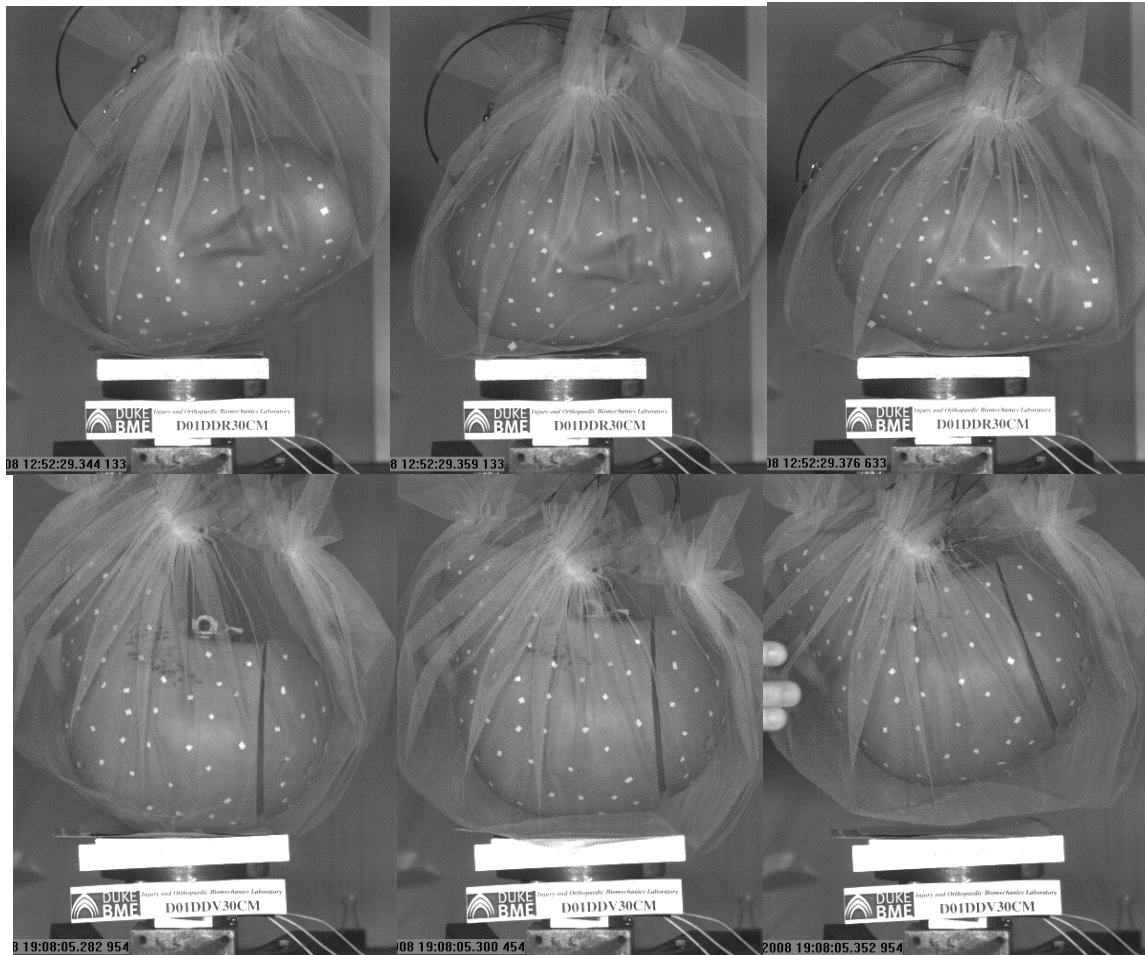


Figure 12: Video footage of the parietal impact (top) and vertex impact (bottom). The parietal impacts had a line of action not aligned with the CG location, causing more rotation and less rebound. The vertex impacts were in the line of action of the CG, which caused more rebound and less rotation. The top row of images shows the kinematics of a Hybrid III 30cm right parietal impact. The head had a maximum rebound of 9mm (top middle) and exhibited a higher absolute average angular acceleration of 2178 radians per second². The bottom row of images depicts the kinematics of a Hybrid III 30cm vertex impact. The head had a maximum rebound of 37mm (bottom right) with a lower absolute average angular acceleration of 710 radians per second². These trends were true for both ATD and adult heads.

Effects of Drop Height

Lastly, drop height was shown to significantly increase the dynamic stiffness (Figure 6 and Table 5). This was true for both the adult and ATD heads. There are two potential reasons for this observed increase. First, head stiffness could be rate-dependent, as the head could behave like a viscoelastic solid [32]. This is plausible, as the response of the soft tissue that surrounds the human skull and the vinyl skin that surrounds the ATD heads have both been shown to be rate-dependent [33, 34]. Secondly, the added energy of the impact causes more compressive deformation of the head during impact. This is demonstrated in Figure 13, as the adult heads had more deformation in the higher drops than the lower ones. As the stiffness increased, the HIC and acceleration similarly increased.

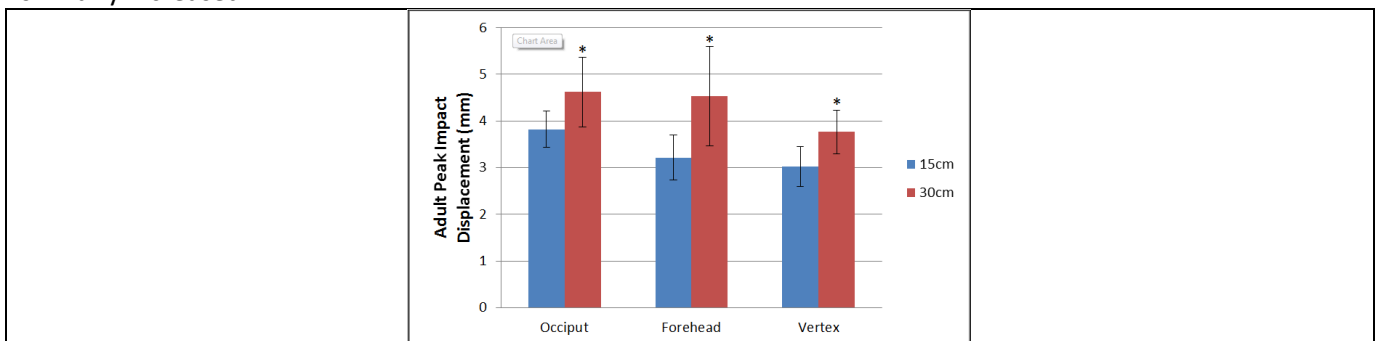


Figure 13: Peak impact displacement for the adult heads. The added displacement and the non-linear stiffening of the head produced higher dynamic stiffness values for higher drop heights. * denotes that the 30cm drop is statistically different from the 15cm drop onto that impact location (student t-test p<0.05).

Limitations

There are limitations to this study. The first limitation was that the heads were dropped with no mandible attached. This prevented any investigation into the head impact being coupled with the jaw. However, the current data with the mandible removed were not statistically different from the Hodgson head drops, for which the mandible was attached [17]. The second limitation is the boundary conditions at the foramen magnum. The head was sealed at the foramen magnum with PMMA, which provided a different boundary condition than a spinal cord and cerebrospinal fluid would. However, the sealed foramen magnum was used to prevent the secondary impact from the intracranial contents impacting the inner skull. Third, this analysis was conducted by examining one-dimensional motion. The other two directions were not analyzed; however, measurements of the shear loading of the drops were consistently less than 3% of the peak force measured in the z-direction, and therefore were not considered significant. Fourth, the average age of the adult heads in this study was 61-years-old. The adult heads in this study are representative of elderly adults, with no representations of adults between the ages of 18 years and 50 years. Lastly, the head impacts in this study were repeated impacts onto the same locations--all of the 30cm head impacts were performed after the head was impacted from 15cm.

V. CONCLUSIONS

The impact responses of the adult Hybrid III onto different impact locations were found to be an adequate representation for adult impacts 30cm and below. The adult Hybrid III was found to have no statistical differences from the adult heads for impact stiffness, peak acceleration or HIC. The impact properties of the ATD heads generally increased with represented age, with the Q3 dummy being the exception. The Q3 dummy consistently produced the highest HIC values of the ATD heads, and produced higher acceleration and HIC values than the adult human heads as well, which is contrary to neonatal data demonstrating that the head acceleration decreases with age [27].

This study demonstrated that impact location and drop height are important factors influencing the response of the head. The impact location was important, because differences in the skull thickness and impact kinematics affected the impact properties. Lastly, the heads responded more stiffly with increased drop height due to non-linear stiffness responses and added energy.

VI. REFERENCES

- [1] Faul, M., Xu, L., Wald, M. M. and Coronada, V. G. *Traumatic Brain Injury in the United States: Emergency Department Visits, Hospitalizations and Deaths 2002-2006*. National Center for Injury Prevention and Control, City, 2010.
- [2] Schneier, A. J., Shields, B. J., Hostetler, S. G., Xiang, H. and Smith, G. A. Incidence of Pediatric Traumatic Brain Injury and Associated Hospital Resource Utilization in the United States. *Pediatrics*, 118483-492 (2006)
- [3] Mertz, H. J. Biofidelity of the Hybrid III Head. *Society of Automotive Engineers* (1985)
- [4] Foster, J., Kortge, J. and Wolanin, M. A biomechanically based crash test dummy. *Proceedings of the Twenty-First Stapp Car Crash Conference* Warrendale, PA, Warrendale, PA, pages 1977.
- [5] FMVSS Standard No. 208; *Occupant crash Protection*. U.S. Department of Transportation, City, 1998.
- [6] Irwin, A. and Mertz, H. J. Biomechanical Basis for the CRABI and Hybrid III Child Dummies. *The Stapp Car Crash Journal*, 41261-272 (1997)
- [7] van-Ratingen, M. R., Twisk, D., Schrooten, M., Beusenberg, M. C., Barnes, A. and Platten, G. Biomechanically Based Design and Performance Targets for a 3-Year Old Child Crash Dummy for Frontal and Side Impact. *Society of Automotive Engineers International* (1997)
- [8] Hubbard, R. P. and McLeod, D. A Basis for Crash Dummy Skull and Head Geometry. *Proceedings of the Symposium on Human Impact Response; Measurement and Simulation*, Warren, MI: General Motors Corporation Research Laboratories, Warren, MI: General Motors Corporation Research Laboratories, pages 129-152 1973.
- [9] Hubbard, R. P. and McLeod, D. G. Definition and Development of a Crash Dummy Head. *Eighteen Stapp Car Crash Conference* 599-628 (1973)

- [10] Messerer, O. *Über Elasticität und Festigkeit der Menschlichen Knochen*, Stuttgart, Germany, 1880.
- [11] Dibb, A. T., Nightingale, R. W., Luck, J. F., Chancey, V. C., Fronheiser, L. E. and Myers, B. S. Tension and Combined Tension-Extension Structural Response and Tolerance Properties of the Human Male Ligamentous Cervical Spine. *Journal of Biomechanical Engineering*, 131, 8, (2009)
- [12] Walker, L., Harris, E. and Pontius, U. Mass, volume, center of mass, and mass moment of inertia of head and head and neck of human body. *Stapp Car Crash Conference* 17th525-537 (1973)
- [13] SAEJ222-1 *SAE J211/1- Instrumentation for impact test part 1: Electronic Instrumentation Society*. Society of Automotive Engineers, 1995.
- [14] Kleinberger, M., Sun, E., Eppinger, R., Kuppa, S. and Saul, R., Head Injury Criteria. pages 12-17, NHTSA Washington D.C, 1998.
- [15] Lehman, A., O'Rourke, N., Hatcher, L. and Stepanski, E. J., One-Way ANOVA with one Repeated-Measures Factor. pages 281-314, SAS Institute Inc. Cary, NC, 2005.
- [16] Hodgson, V. R. Tolerance of the facial bones to impact. *Am. J. Anat.*, 120113-122 (1967)
- [17] Hodgson, V. R. and Thomas, L. M. Comparison of head acceleration injury indices in cadaver skull fracture. *Proceedings of the Stapp Car Crash Conference*, pages 190-206 1971.
- [18] Nightingale, R. W. *The Dynamics of Head and Cervical Spine Impact*. Dissertation, Duke University, Durham, 1993.
- [19] Yoganandan, N., Zhang, J. and Pintar, F. A. Force and Acceleration Corridors from Lateral Head Impacts. *Traffic Injury Prevention*, 5, 4, 368-373 (2004)
- [20] Coats, B., Margulies, S. S. and Ji, S. Parametric Study of Head Impact in the Infant. *Stapp Car Crash Journal*, 511-15 (2007)
- [21] Zhang, L., Yang, K. H. and King, A. I. Biomechanics of Neurotrauma. *Neurological Research*, 23144-156 (2001)
- [22] Prange, M. T., Luck, J. F., Dibb, A., Van Ee, C. A., Nightingale, R. W. and Myers, B. S. Mechanical Properties and Anthropometry of the Human Infant head. *The Stapp Car Crash Journal*, 48 (2004)
- [23] Nightingale, R. W., McElhaney, J. H., Richardson, W. J. and Myers, B. S. Dynamic Responses of the Head and Cervical Spine to Axial Impact Loading. *Journal of Biomechanics*, 29, 3, 307-318 (1996)
- [24] Pintar, F. A., Sances, A., Yoganandan, N., Reinartz, J., Maiman, D. J., Suh, J. K., Unger, G., Cusick, J. F. and Larson, S. J. Biodynamics of the total human cadaveric cervical spine. *Proceedings of the 34th Stapp Car Crash Conference*, pages 55-72 1990.
- [25] Mertz, H., Jarrett, K., Moss, S., Salloum, M. and Zhao, Y. The Hybrid III 10-year-old Dummy. *Stapp Car Crash Journal*, 45319-328 (2001)
- [26] Melvin, J. W. Injury Assessment Reference Values for the CRABI 6-Month Infant Dummy in a Rear-Facing Infant Restraint with Airbag Deployment. *SAE Technical Paper Series* (1995)
- [27] Prange, M., Luck, J., Dibb, A., Ee, C. V., Nightingale, R. and Myers, B. Mechanical Properties and Anthropometry of the Human Infant Head. *Stapp Car Crash Journal*, 48279-299 (2004)
- [28] Getz, B. Skull Thickness in the Frontal and Parietal Regions. *Acta morphologica Neerlando-Scandinavica*, 3221-228 (1960)
- [29] Ishida, H. and Dodo, Y. Cranial Thickness of Modern and Neolithic Populations in Japan. *Human Biology*, 62, 3, 389-401 (1990)
- [30] Lynnerup, N. Cranial thickness in relation to age, sex and general body build in a Danish forensic sample. *Forensic Science International*, 11745-51 (2001)
- [31] Finan, J. D., Nightingale, R. W. and Myers, B. S. The Influence of Reduced Friction on Head Injury Metrics in Helmeted Head Impacts. *Traffic Injury Prevention*, 9, 5, 483-488 (2008)
- [32] Stronge, W. J., *Direct Impact of Viscoelastic Bodies*. pages 86-93, Cambridge University Press Cambridge, 2000.
- [33] Wood, G. W., Panzer, M. B., Bass, C. R. and Myers, B. S. Viscoelastic Properties of Hybrid III Head Skin. *SAE International Journal of Materials and Manufacturing*, 3, 1, 186-193 (2010)
- [34] McElhaney, J. H., Stalnaker, R. L., Estes, M. G. and Rose, L. S. Dynamic Mechanical Properties of Scalp and Brain. *Proceedings of the Annual Rocky Mountain Bioengineering Symposium*, pages 67-73 1969.